JAAS

Accepted Manuscript

This is an *Accepted Manuscript*, which has been through the Royal Society of Chemistry peer review process and has been accepted for publication.

Accepted Manuscripts are published online shortly after acceptance, before technical editing, formatting and proof reading. Using this free service, authors can make their results available to the community, in citable form, before we publish the edited article. We will replace this *Accepted Manuscript* with the edited and formatted *Advance Article* as soon as it is available.

You can find more information about *Accepted Manuscripts* in the Information for Authors.

Please note that technical editing may introduce minor changes to the text and/or graphics, which may alter content. The journal's standard Terms & Conditions and the Ethical guidelines still apply. In no event shall the Royal Society of Chemistry be held responsible for any errors or omissions in this *Accepted Manuscript* or any consequences arising from the use of any information it contains.

ROYAL SOCIETY OF CHEMISTRY

www.rsc.org/jaas

A table of contents entry

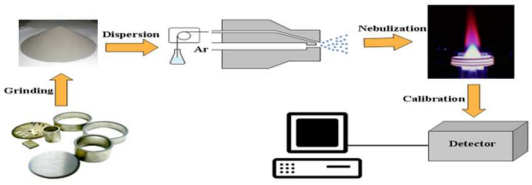

The current state of research on slurry nebulization in plasmas for the analysis of advanced materials is thoroughly surveyed.

Slurry Nebulization in Plasmas for Analysis of Advanced Ceramic Materials

Zheng Wang[a] and Pengyuan Yang[b]

[a]*Shanghai Institute of Ceramics, Chinese Academy of Sciences, Shanghai 200050, China. E-mail: wangzheng@mail.sic.ac.cn*

[b]*Department of Chemistry, Fudan University, Shanghai 200433, China. E-mail: pyyang@fudan.edu.cn*

Abstract: Slurry nebulization in plasmas has advantages of simplicity, high speed, low cost, minimized analyte loss, and low risk of sample contamination, but it has not been very widely adopted. However, the study of advanced ceramic materials has recently renewed enthusiasm for this technique. In this paper, the current state of research on slurry nebulization in plasmas for the analysis of advanced materials is thoroughly surveyed. Sample preparation, sample characterization, and modifications of the instrumentation necessary for slurry nebulization are reviewed, along with calibration procedures and studies on fundamental issues. Finally, the applications of this method to a variety of advanced materials are summarized, and the outlook for this method is discussed.

1. Introduction

The development of structural and functional ceramics for modern industrial applications and electronic devices requires interdisciplinary investigations in the fields of mineralogy, materials science, materials processing, and materials testing in general, as well as in analytical science in particular[1]. Advanced ceramics are synthesized from pure or alloyed oxides, nitrides, carbides, and borides with rigidly defined structures, shapes, and chemical compositions. In particular, oxide-based materials (aluminium oxide (Al_2O_3), titanium dioxide (TiO_2), zirconium oxide (ZrO_2)), non-oxide-based nitrides, carbide materials (aluminium nitride (AlN), titanium nitride (TiN), silicon carbide (SiC), silicon nitride (Si_3N_4), boron carbide (B_4C)), and their chemical compounds have all been used as raw materials for advanced ceramic synthesis.

The fantastic properties of advanced ceramic materials, such as their high-temperature stability, strength, wear resistance, corrosion/oxidation resistance, and electrical optical and/or magnetic properties, rely greatly on their chemical composition and purity.[2] In particular, advanced ceramics are usually of high purity, and in a number of cases even a trace level of impurities severely affects ceramic performance.[3,4] Furthermore, small amounts of dopants, sintering aids, and other additives are normally spiked into these ceramics to improve their processing and ultimate properties.[5] Therefore, the chemical composition of the powders used

for the production of advanced ceramics must be determined with a high precision, down to trace concentrations, for manufacturing control, property improvement, failure prevention, and quality assurance. Furthermore, because the chemical composition of advanced ceramics, especially the impurities, should be exactly controlled for their continuing high quality, analysis of not only the raw material but also the sintered material is required.

Therefore, powerful analytical methods and strategies are required to determine the main elements and the impurities of raw and sintered materials. Since many elements have important effects on the properties of advanced ceramics, only methods with a high multi-element capacity should be applied, such as inductively coupled plasma optical emission spectrometry/mass spectrometry (ICP-OES/MS). Traditionally, samples have been prepared as solutions using digestion steps such acid dissolution or fusion. This facilitates introduction, calibration, and homogenization. However, advanced ceramics are difficult to digest even by microwave-assisted digestion.[6] Alkali fusion procedures have the disadvantages of high reagent blanks due to the fluxes and large dilution factors, both of which lead to a sensitivity decrease. Meanwhile, some elements may not be detected, especially trace elements. Methods based on, for example, fusion and digestion using acids can result in incomplete dissolution of the sample, evaporative losses of the more volatile elements, and contamination problems. For these reasons, sample preparation for advanced ceramic materials is still the Achilles' heel of ICP-OES/MS as a microquantity analysis technique. The direct introduction of solids or slurries into plasmas would circumvent these difficulties and markedly reduce the sample preparation time by combining the matrix destruction and analyte atomization and excitation into a single step. The solid samples can be introduced into the plasma using a number of well-established techniques.

Direct sample insertion with a graphite rod as a support and a sample elevator is commonly used to introduce a solid into an ICP.[7] The inductive heating of the carbon vaporizes the sample directly into the plasma. Direct insertion may provide low limits of detection and a wide dynamic range, but it suffers from the high temperature stability (i.e., high vaporization temperature) of refractory materials and ceramics consisting of stable carbide-forming elements. Another important requirement is the need for closely matching standards. Because of these practical limitations, direct introduction of powders into the ICP-OES has not been exploited successfully to its full potential for routine analysis in spite of its many import advantages.[8,9]

Laser ablation (LA) is increasing in popularity as a method of direct solid sample introduction. Specially, LA coupled with ICP-MS has been become a well-established, powerful, rapid, and sensitive method for analysing trace elements without extensive sample preparation.[10-12] However, the lack of appropriate standards or certified reference materials for a wide variety of

samples of interest is the most important restriction for quantitative analysis by LA-ICP-MS. For ceramics in particular, suitable standards are often not available, resulting in a need of for calibration methods. LA-ICP-MS also suffers from non-stoichiometric effects during sampling, aerosol transport, vaporization, atomization, and ionization in ICP, which are collectively described as elemental fractionation. Furthermore, quantitative analysis of powdered materials like advanced ceramic powders is especially difficult. For these reasons, laser ablation has usually been applied to compact ceramic samples but not to ceramic powders.

Electrothermal vaporization (ETV) has often been combined with other techniques such as ETV-ICP-OES or ETV-ICP-MS to provide a high sample introduction efficiency, low sample volume, high absolute detection power, and the possibility of removing certain sample components before the vaporization step or of using chemical modifiers.[13,14] However, the condensation step during transport to the plasma, memory effects, soaking of the sample into the furnace material, blanks, chemical reactions, and spectral interference caused by the furnace material can limit the applicability of this technique. Generally, it is difficult to completely vaporize ceramic powder from the ETV device because of its high thermal stability.

Another approach to solid sample introduction is slurry nebulization, which involves the nebulization of (usually aqueous) suspensions of fine powders into the ICP. This technique also requires only simple preparation procedures.[15–17] Extreme temperature conditions are usually utilized in ICP, which is a tremendous potential advantage that has been neglected in other methods. In general, the plasma is only used to ignite the light source. However, the high-temperature environment could also be used to thermally decompose samples into atoms or ions. Therefore, nebulization of suspensions of powdery samples and subsequent introduction of the nebulized samples into the ICP torch, i.e., slurry nebulization, has been received particular attention in the past two decades.[16,17] Because of the similarities between the rheological properties of suspensions and solutions, the technique is simple to operate, and only a few instrumentation modifications (nebulizer and spray chamber) are required. In addition, it can remarkably reduce the analysis time by combining the sample decomposition and analyte atomization and excitation into a single step.

Fig. 1 shows the number of the publications on slurry nebulization into plasmas published from 1996 to 2013 and reflects its popularity as an alternative to conventional aqueous sample introduction. It is interesting to see that the number of published papers has not varied drastically over the past 20 years, although the number of publication has decreased in the last several years. Slurry nebulization techniques have been successfully applied in many different fields such as bioorganic and inorganic materials analysis, and many of the early difficulties in achieving a

homogeneous and stable dispersion have been overcome. It has also shown advantages such as simple implementation, low cost, the requirement for only slight instrument modification, and easy calibration using aqueous solutions in a way similar to solution nebulization. The aim of this article is to survey the current status of slurry nebulization in ICP with a special focus on the work on advanced ceramic materials in latest twenty years. The outlook for this method is also discussed.

2. Slurry Preparation

The most critical step for successful analysis of advanced ceramic materials using ICP is probably the slurry sample preparation, which can determine the analysis time, trueness, precision, and reliability of the analysis results. The ideal slurry sample should be highly stable and homogeneous, and the slurry particle size should be sufficiently small.[15] In general, the principal steps in sample preparation include sample grinding, dispersion reagent addition, and characterization of the slurry homogeneity and stability. These steps are each discussed in the present work.

2.1 Grinding methods

The particle size is the limiting parameter for efficient slurry nebulization, and the maximum particle size of the slurry must be such that any single solid particle can occupy an aerosol droplet. To achieve a particle size distribution that would yield results similar to those of an equivalent equimolar aqueous solution, a wide range of grinding techniques have been employed. Technically, the slurry particles have to be sufficiently small (down to the nanometre scale) to be able to be analysed using ICP. Even if the ceramic materials are in a powder form, they may still require grinding to meet the requirements for slurry nebulization. Ebdon *et al.*[16] reported that during slurry nebulization, the particle size in a slurry for ceramic analysis should be smaller than 5–10 μm. Their rigorous study showed that the slurry particles larger than 5 μm (in some reports 2 μm) could not reach the plasma, which resulted in signal loss. Wang *et al.*[18] suggested that the particle size in some ceramic analyses should be reduced to the submicron level, because otherwise there would be a negative deviation in the analytical results due to the incomplete evaporation of the slurry particles.

Most ceramics have a high hardness and are therefore difficult to grind. The attrition materials used in mills and grinders such as zirconium and tungsten carbide have a Mohs value comparable to those of most ceramics, which can lead to poor grinding efficiency and easy contamination if a long grinding period is used. A wide range of grinding methods has been used

for slurry preparation for direct analysis in ICP. The main methods utilized for ceramic powders reported in the literature are the bottle and bead method, vibration mill, and puck-type grinder with tungsten carbide utensils. Table 1 lists the various mills and size reduction methods that have been used to date, with varying degrees of success, to grind a wide range of materials. The obtained particle size ranges are also tabulated. The choice of grinding or milling agent is also important and will affect the analytical accuracy. In particular, the grinding material should be harder than the material being ground and should not contain elements that will interfere with the analysis.

The bottle and bead method [19-21] has been widely used to prepared slurries from a wide variety of ceramic materials, as shown by Table 1. Approximately 0.1 to 1 g of sample is weighed into 30 mL polypropylene bottles, and then 10 g of zirconia beads and an aqueous dispersing agent are added. Afterward, the bottles are sealed and shaken on a mechanical laboratory shaker for the amount of time required to produce a slurry in the appropriate size range, often overnight for convenience. The resultant finely ground slurry can then be transferred to a calibrated flask through a coarse sieve that retains the grinding material and diluted to the desired volume with a dispersant. This technique is inexpensive and offers the advantage of grinding a number of samples simultaneously, depending on the type of flask shaker used.

Vibration mills[19,22,23] consist of a torus-shaped or cylindrical shaped shell. The solid is contained in the shell, together with the beads for grinding, and vibrated. The grinding material and sample collide with each other and the shell, resulting in the breakdown of solid particles. The mills can be run dry or wet, and steel, agate, and tungsten carbide can be used as grinding materials.

A puck-type grinder reduces the particle size through the action of a spinning puck and a ring inside a grinding container.[24,25] The grinding container may be made with materials resistant to abrasion, e.g., hardened steel, tungsten carbide, agate, or alumina ceramic. Alumina ceramic in particular resistant to abrasion and lightweight, as it is almost pure aluminium oxide with trace amounts of silicon, calcium, and magnesium, although it is brittle.

Isoyama *et al.*[26] investigated the use of an ultrasonic grinding technique for direct analysis of slurries by ICP-OES. In this method, a sample block was ground with the same sample pestle fixed on an ultrasonic horn along with a sample coarsely crushed in water for 10 min. In result, 10 to 20 mg of the finely ground sample (0.5 to 0.7 mm of mean particle size) was obtained. Reduced contamination from the grinding tools was achieved even though very fine samples of less than 1 mm were obtained for sintered ZrO_2-Al_2O_3 ceramic materials.

Recently, the jet-milling method has been used to further decrease the particle size.[22] In

general, jet milling systems mainly consist of a grinding chamber and a classifying chamber. After entering the grinding chamber, the raw particles are accelerated by means of a jet stream of carrier gas, and extremely high-energy mechanical impact collision occurs among particles and between particles and rigid obstacles. As a result, the powder particles can be efficiently smashed and refined. After grinding, the particles are carried out by the carrier gas and flow up to the classifier chamber with a rotating rotor, where classification takes place.

However, advanced ceramic materials with high measure of hardness (MOH) values may still be difficult to grind. For example, the attrition materials used in mills and grinders such as zirconia and tungsten carbide may have comparable MOH values, resulting in poor grinding efficiencies and even contamination if long periods are employed for size reduction. In general, the ceramic sample should be ground for particle size reduction. Several points should be considered in particle size reduction step: the type of mill and grinding methods, milling container, milling speed, milling time, and the desired particle size and particle size distribution.[28]

2.2 Dispersion of the slurry

Preparing slurries in an aqueous solution alone is unsuitable for the majority of samples owing to flocculation effects, which result in rapid sedimentation of the finely powdered material. It is therefore essential to prepare a stable and homogeneous slurry that will yield a stable, homogeneous aerosol for introduction into the plasma to obtain accurate and precise analytical results. This is achieved by employing stabilizing agents, which are commonly termed dispersants or surfactants.

Slurry stabilization can be described by the DLVO (Derjaguin and Landau, Verwey and Overbeek) theory.[29,30] In this approach, the electrostatic interactions between the charged particles caused by their surface electrical potential, the so called zeta potential, are calculated. The effects of van der Waals attractions and electrostatic repulsions due to the double layer of counter ions are then both considered. Slurry flocculation occurs when the van der Waals attraction overweighs the electrostatic repulsion. This slurry stabilization mechanism can be influenced by the surface properties of the sample powder to be analysed. Therefore, some preparation conditions, such as the medium pH and the type and amount of dispersants, should be experimentally optimized in order to prepare a stable and homogeneous slurry.

Many reports[15,18,26,31,32] have discussed the effects of the pH of aqueous ceramic suspensions on colloidal stability as well as the measurement precision in slurry nebulization ICP-OES analysis. Farinas *et al.*[15] published an excellent study regarding the colloidal stability of ceramic

suspensions for slurry nebulization in ICP-OES. They reported a case study using alumina slurries with different pH conditions and stabilization agents. The paper discusses the different types of stabilizing additives available for ceramic suspensions and also their best uses. The authors explain the electrostatic stabilization mechanism in detail and conclude that in a ceramic suspension, H^+ and OH^- ions determine the potential. In the case of Al_2O_3, the charge on the surface of any slurry particle is negative, resulting in the attraction of protons to the surface and creating a proton concentration gradient from the particle surface to the liquid. Conversely, the OH^- ion concentration is decreased near the surface of the particle and increases with distance from the surface. A charged layer, known as the electrical double layer, is formed because of the potential gradient. According to the Nernst equation, the surface potential of the particle can be changed by changing the concentration of the potential-determining ion, and the relative amount of ions adsorbed on the surface of the slurry particle will change as a result.

If the surface of the solid in the preferred liquid carrier is lyophobic, the powder will be difficult to disperse, whereas if it is lyophilic, the powder will disperse easily. To obtain a suitable dispersion of lyophobic particles,[7] stabilization agents are added to wet the surface, so that the particles become lyophilic. There have been few in-depth studies regarding the stabilizing effect of dispersants. At a particular concentration of the potential-determining ion, the positive and negative surface activities will be equal, and the overall potential at the surface of the particle will be zero. In this scenario, no double layer will exist, and agglomeration of the particles will occur at a concentration known as the isoelectric point (IEP). The addition of a dispersant causes the zeta potential to change and ultimately acts to stabilize the slurry. Triton X-100 was found not to stabilize alumina slurries, and no real dispersion was achieved with Kodak photoflow in glycerol. PKV-5088 was unable to prevent sedimentation of alumina despite being commonly used to disperse non-oxide ceramics. Three dispersants, Dolapix PC-33, Darvan-C, and Darvan-7, were found to produce the desired dispersion of an alumina slurry. The intensity and precision of the ICP-OES measurement were found to be directly related to the stability offered by the dispersant system. Wang *et al.* prepared an SiC slurry with polyethylene imine (PEI),[19] AlN suspensions with polyacrylate amine (NH_4PAA) or PEI,[18] a TiO_2 slurry with NH_4PAA,[24] and TiN suspensions with NH_4PAA or PEI.[25] Before nebulization, each slurry was agitated in an ultrasonic bath for 15 min to ensure stable dispersion.

The authors found that the dispersant may yield the required stability through an electrostatic stabilizing mechanism by (i) controlling the pH (using potential determining ions), (ii) using inorganic electrolytes, or (iii) using a polyelectrolyte whose long-chain polymers adsorb on the surfaces of the particles and prevent contact between them. Various dispersants used in slurry

preparations are summarized in Table 2, including glycerol, sodium hexametaphosphate applied alone or mixed with monoisopropanolamine, NH_4PAA, and PEI.

2.3 Slurry concentration

In direct sample-introduction systems, the slurry concentration is important because it strongly affects the overall sensitivity. Very dilute slurries may cause a decrease in precision, whereas at high slurry concentrations the plasma stability and nebulization efficiency of the sample may be significantly reduced. The upper limit of the concentration depends on the sample matrix being analysed.

Zachariadis *et al.*[43,44] conducted some preliminary experiments using a cyclonic spray chamber combined with a Babington-type nebulizer. Slurry solutions with concentrations up to 10% (m/v) were tested. They found that slurry solutions with concentrations up to 2.5% (m/v) can be easily aspirated without any significant influence of the concentration on the plasma or baseline stability.

The effects of the ceramic suspension viscosity should also be taken into consideration for very concentrated slurries, because viscosity is known to influence the aspiration rate and thus to alter the nebulization efficiency. As a general rule, concentrated ceramic suspensions have very poor rheological properties, especially for nanosized powders. The slurry cannot flow when the solid content reaches 30% (m/v) at any pH value. Wang *et al.*[45] prepared a unique SiC slurry sample containing 30 wt% solid in order to detect the trace elements in SiC powders. However, the viscosity of the suspension was only 40 mPa·s after the dispersant was added. Thus, the flowability was significantly improved to near that of an aqueous solution, and a linear signal enhancement was observed up to a slurry concentration of approximately 20% (m/v).

From these results, it can be concluded that the effects of viscosity and non-Newtonian rheological phenomena should be considered for very concentrated slurries. In addition, whereas conventional acid dissolution procedures produce solutions with a 1% sample content, the ability to use slurries with a sample content of 20% or more has clearly yielded major advantages in trace analysis.

3. Slurry characterization

In the direct analysis of a slurry, it is necessary to control the stability and homogeneity of the slurry to produce a reliable aerosol for introduction into the plasma and thus provide precise and accurate analytical results. Furthermore, even more caution is needed for the analysis of ceramic powders using techniques for slurry nebulization into plasma, because the transport and

nebulization efficiencies are strongly influenced by the stability and homogeneity of the aqueous slurries under these conditions.

3.1 Particle size and its distribution

The stability and homogeneity of the slurry are influenced by the particle size. Recently, various methods have been developed to measure the particle size and its distribution in slurries, and the method adopted for measurement of the particle size generally depends on the available instrumentation.

Photosedimentometry combines photoelectric measurement and gravitational settling of particles. A narrow beam of light is passed through the slurry and onto a photocell. As particles begin to fall and leave the light beam, they are replaced by particles settling from above. The attenuation of the beam of light is directly related to the surface area of the particles in the light beam, and from this relationship, the particle size distribution can be determined. The method is simple and the instrument is inexpensive, and thus photosedimentometry is widely employed for particle determination.[18,19,24]

For more sensitive analysis, SEM is commonly used to measure the mean particle size in a slurry, as well as the dispersion stability of the slurry.[18,19,25] The particle size and distribution of AlN can be observed on the SEM screen (Fig. 3). The dispersing effect of the PEI can also be verified by comparing the SEM micrographs of sediments. Large flocs are observed in the sediments of suspensions without PEI, while particles of the sediments with 2 wt% PEI are well dispersed and not associated with each other.[18] SEM has a large depth of focus and can yield significant information about the size, shape, and surface characteristics of the particles. However, only information on spatially confined areas can be obtained.

Laser diffraction methods[18,19,46] can also be used to assess the dispersion efficiency of a slurry. Diffraction of light, which can be thought of as the bending of light waves, occurs at the surfaces of the particles because of slight differences in the path lengths of the light waves created upon interaction with the particle surfaces. Laser diffraction methods are rapid, do not require the use of dispersants, and can be employed with a range of slurry concentrations. However, the instrumentation required is relatively expensive. Isoyama *et al.*[26] measured the mean particle sizes of ground sample powders using a laser particle size analyser and SEM images. The mean diameter of the sample obtained by grinding the 0.25–0.5 mm coarsely crushed sample fraction was less than 1 mm, and the particle size distribution curve was extremely sharp.

3.2 Slurry stability

As discussed above in section 2.2 regarding the dispersion of the slurry, the stability of the slurry can be theoretically explained and characterized by the zeta potential, which is a measure of the electric field resulting from the particle surface charge. As mentioned, the zeta potential can be altered by the pH and/or surfactants, and the zeta potential becomes zero, meaning that the surface charge disappears, at a specific pH value called the IEP. At the IEP, the suspended particles would agglomerate rapidly owing to the absence of the repulsive force. Thus, the greater the absolute value of the zeta potential, the more stable the slurry is. Wang *et al.*[19] studied the relationship between the zeta potential of an SiC slurry and pH, and Broekaert *et al.*[36] analysed similar relationships for ceramic materials (Al_2O_3, SiC, and ZrO_2) by ICP-OES. The refractory materials were added in water and sonicated during 10 min in an ultrasound bath. A surfactant was not needed to stabilize the slurry, because the ultrasonic agitation guaranteed homogenization.

The additives adsorbed onto the particle surface create a large energy barrier to prevent the colloid particles from flocculating. Because each individual material has different surface properties, as a rule, an appropriate dispersant must be selected on a case-by-case basis.[18,23-25] Slurries of the same ceramic material with different particle sizes usually require different amounts of dispersant. Nanosized powders have larger specific surface areas than submicron powders and thus require more additive to disperse the particles.[18,23-25,45] Clearly, the concentration of a dispersant must be controlled, because excess dispersant is detrimental to the slurry stability and can cause coagulation.[18]

Wang *et al.*[19,25] studied the stability of slurries by measuring the relationship between ICP-OES signal intensity and time. The submicron SiC slurry with no dispersant at the IEP (zeta potential is zero) displayed unstable properties. The normalized line intensities of the matrix Si and the Al and Fe impurities obviously decreased with time. In contrast, the slurry with 2.0 wt% PEI as a dispersant, the zeta potential of which was far from zero, displayed relatively stable signal intensities.[19]

3.3 Viscosity determination

The viscosity influences both the aspiration rate and the nebulization process. Good fluidity of the slurry, which implies a low viscosity, improves the nebulization efficiency. However, there has been little research on the viscosity in terms of its influence on the nebulization. Farinas *et al.*[15] reported on the rheology of ceramic slurries and discussed the basic concept of rheology. Wang *et al.*[45] prepared a slurry for viscosity measurement with the help of ultrasonic stirring, followed by magnetic stirring for 20 min. The viscosity was determined using a cylindrical

measurement system on a rotational viscometer. The viscosity measurements for all slurries were conducted at 25 ℃ within 30 min after preparation. To eliminate the artefacts from different treatments during the filling procedure, the samples were presheared for 3 min, followed by 5 min of rest. The viscosity can be kept very low even when the SiC slurry concentration is as high as 30% (m/v) when 2.0% PEI is added and the medium has pH 4. In fact, such a high-concentration SiC slurry can be normally nebulized for ICP-OES analysis without any problem.

4. Slurry sample introduction system

As mentioned previously, because of the similarity between the rheological properties of suspensions and solutions, slurry nebulization in plasmas is simple to achieve with only a few instrumentation modifications in the nebulizer and spray chamber.

Although there are many similarities, there exist some differences in rheological properties between suspensions and solutions. The primary difference is that the suspensions contain particles. Theoretically, the solution sample can be divided infinitely in the nebulization process, whereas the slurry particles cannot be divided. Therefore, the sizes of aerosol droplets must be larger than the slurry particles, and clogging will occur when a conventional concentric pneumatic nebulizer is employed. Thus, the most critical consideration in the design of a nebulizer for slurry nebulization is to prevent clogging. Fig. 2 shows the different nebulizers used for the slurry nebulization into plasma.

Many nebulizers suited to slurry samples were reported in the early articles on this topic. The most popular designs for handling slurries are based on the V-groove Babington-type nebulizer.[33,46,47,48] The slurry sample flows along a V-groove that has a small orifice through which the carrier gas blows out at high flow rates. This causes the sample to shatter into an aerosol of small droplets. The high pressure of the argon gas ensures efficient nebulization and prevents blocking of the small orifice.

The Ebdon nebulizer[49-51] is a commonly used V-groove variation of the Babington nebulizer. It has been shown to exhibit excellent performance for slurry nebulization and has a robust one-piece design. The diameter of the gas orifice is 0.2 mm to allow a high-velocity gas flow to be used for nebulization.

However, in recent years, there have been few reports on nebulizer designs for slurry nebulization, probably because many commercial nebulizers are available in the market. Three different nebulizers were tested by Kollander *et al.*,[52] including glass expansion concentric (GEC), cross-flow, and Burgener T2100 nebulizers. They all performed roughly equally well in

terms of the quantitative results obtained for the slurries, but the GEC nebulizer yielded better sensitivity (larger slope of the calibration curve) for all elements. The cross-flow and Burgener T2100 nebulizers each yielded about the same sensitivity when the same instrument settings were used. In particular, the GEC nebulizer yielded about 1.4 to 2.5 times higher sensitivity than the Burgener T2100 nebulizer. The GEC nebulizer is known to create a very fine mist with small droplets, whereas the Burgener nebulizer allows larger droplets to form because of its wider inner diameter. These larger droplets are partly filtered by the spray chamber, and consequently less analyte reaches the plasma, resulting in a lower sensitivity. In addition, a slightly lower Mg content was observed when the cross-flow nebulizer was used, which indicates a higher matrix load in the plasma than is obtained with either the GEC or Burgener nebulizer. Increases in plasma load usually lead to decreases in temperature and thus decreases in sensitivity due to reduced atomization and excitation.

The spray chamber has the same importance as the nebulizer in slurry nebulization. After passing though the nebulizer outlet, the aerosol droplets are separated based on their different sizes. Most large droplets are removed to drain, while a small fraction of droplets are carried to the plasma torch. According to the Ebdon's study,[16] only approximately 1%–2% of the samples can reach the plasma.

Ebdon *et al.*[46] reported that good recovery efficiency could be obtained by using a laboratory-constructed double-pass spray chamber made of glass. The double-pass design is used to eliminate the considerable dead volume in a single-pass spray chamber, which improved the recovery efficiency for a sewage sludge analysis. There are also many chamber designs available for slurry nebulization. Williams *et al.*[53] used a single-pass water-cooled spray chamber worked at 13 °C. The cold spray chamber reduced the noise by lowering the vapour loading in the plasma and therefore improved the precision. Just recently, a commercial reduced-volume Sturman–Masters-type spray chamber made of poly(tetrafluorethylene) has come on the market and has been used by many researchers.[18,19,22-25,45,46]

Zachariadis *et al.*[43,44] examined different configurations of the spray chamber and nebulizer for direct aspiration of slurry samples into the plasma. As mentioned above in the discussion of slurry concentration in section 2.3, they found that slurry solutions with concentrations up to 2.5% (m/v) can be easily aspirated without significant influence of the concentration on the plasma or baseline stability by using a Babington-type nebulizer combined with a cyclonic spray chamber. The combination of a Scott-spray chamber and a cross-flow nebulizer had a lower concentration tolerance: slurries containing only up to 1.0% (m/v) powder could be sufficiently aspirated. However, the combination of a cross-flow nebulizer with a double-pass spray chamber

exhibited better performance in terms of overall precision.

5. Optimization

Procedures for the optimization of the operating variables are increasingly being used to enhance the sensitivity and performance of the analysis of slurries using plasma. Some slurries may be difficult to volatilize and atomize, which could be overcome through the optimization of the plasma conditions.

Zaray *et al.*[39] used three-dimensional plots to identify the optimum rf power (0.8 kW) and aerosol gas pressure (2 bar) for the plasma for determination of Al, Ca, Fe, and Mg in silicon nitride powder. At the optimum conditions for the elemental analyses, the atomization efficiencies ranged from 77% to 100%.

Gervais and Salin[38] optimized their procedure for the ICP-OES analysis of slurries using a heated sample-introduction system. Simplex optimization was performed to optimize the viewing height and temperature. The signal-to-blank ratio for six elements was used as the criterion of merit, and a variation of 5% between the five best vertices was used as an indicator of the optimum being found. The simplex method was also used for the optimization of the forward powder, sample uptake rate, nebulizer gas pressure, plasma gas flow rate, and viewing height for the determination of Al in ZrO_2 slurries.

The thermodynamic properties of the ICP itself can be altered by modifying one or all three of the gas flows used (i.e., N_2, He, or O_2). The excitation temperature has been measured to be around 5500 K for a 1.5 kW Ar plasma, but it increases to 6800 K upon addition of 5% O_2. Identical mixed gas plasmas have been used to enhance the sensitivity of ICP-OES analysis by eliminating particle size and sample composition effects.

Xhoffer *et al.*[54] investigated the effect of the addition of N_2 and O_2 to the plasma gas flow on the exhaust particles during the analysis of silicon carbide by ICP-OES. Both N_2 and O_2 were found to have no effect on the shape or morphology of the submicron aerosols. However, O_2 appeared to change the chemical composition of the exhaust SiC particles, whereas N_2 did not.

6. Calibration techniques

The calibration of the instrument is the most difficult step in the ICP-OES analysis of ceramic slurries. The major problems caused by the presence of solid particles during the direct analysis of slurries by ICP are as follows: (i) the analyte in the slurry must be physically transported into the plasma with the same efficiency as the solution, and (ii) particle-plasma interactions give rise to interference effects that are influenced by the size and chemical composition of the solid

particles.

6.1 Use of standard slurries

Calibration with slurries prepared from standard reference materials is the ideal method.[19,55] Standard suspensions are prepared by homogenizing a known amount of the reference materials. However, the use of standard slurries for calibration is problematic because few ceramic standard reference materials meet the requirements for routine ceramic analysis. Furthermore, the standard reference material should be strictly matched with the analytical sample in terms of composition, densities of elements, and particle size distribution, which is often difficult. Nevertheless, Fernandez *et al.*[55] used a reference slag for the determination of a range of elements. A range of geological standard reference materials have also been made from materials including SiO_2-rich granites, marine sediments, and coals.

6.2 Use of aqueous standards

For a slurry to be efficiently nebulized, vaporized, and atomized, the particle size distribution is crucial. When the introduced slurry is completely desolvated by evaporation and the mean particle size less than 5 μm,[56] simple aqueous standards can be used to establish the calibration curves, because the atomization process experienced by the slurry particles is the same as that experienced by aerosols. Wang *et al.* showed that nanosized TiO_2,[24] AlN,[18] TiN,[25] and SiC[45] ceramics can meet the above requirements, so aqueous standards can be used for calibration. Totland *et al.*[57] used aqueous calibration standards for the analysis of geological samples by ICP-MS.

6.3 Use of standard additions

In the slurry technique, simple aqueous standards can be used for the standard addition method of calibration. However, this technique assumes identical transport characteristics between solutions and slurries. It was employed by Lobinski[42] for the ICP-OES analysis of ZrO_2. Similarly, Zaray[39] analysed silicon nitride powder by using the standard addition method along with a multi-element aqueous stock solution. Marjanovic *et al.*[58] proposed a simplified generalized standard addition method (GSAM) for the analysis of cement, gypsum, and basic slag using ICP-OES with slurry nebulization. The GSAM is an extension to the conventional standard addition method in which both the sample mass and the added amount of standard solution are varied. Furthermore, Santos *et al.* [21] direct analysis of clay and refractory materials slurries by ICP-OES using the GSAM.

6.4 Use of an internal standard

The analytical trueness and precision have also been markedly improved by employing an internal standard such as yttrium and scandium in ICP-OES. In ICP-MS, aluminium has been used with success.[59] Ebdon *et al.*[49] reported the use of two internal standards in ICP-MS analyses, rhodium for a semiquantitative analysis and indium for a fully quantitative study. The internal standard can be used to compensate for reduced transport efficiency and inefficient atomization, particularly in the analysis of refractory elements in geological samples and ceramics. However, it is important that any internal standard used in aqueous solution is compatible with the selected dispersant.

The intrinsic internal standard (IIS) method is efficient for correcting for differences in transport and evaporation efficiencies between the slurry and the aerosol.[16] In particular, for the analysis of ceramic samples with large particles (micron or submicron sizes) or high boiling points, the IIS method must normally be used to obtain a correction factor for calibration. The matrix element, for instance, the titanium in TiN, can be selected as the IIS.[25] The correction factor is calculated by measuring the spectral signals of the IIS element and calculating the element concentrations in both the aerosol and slurry.

6.5 Use of empirical correction factors

Alternative calibration methods have also been used for the analysis of slurries to improve the analytical accuracy. For example, empirical correction factors have been employed[34] when the intensity of an elemental line for a slurry analysis is lower than that obtained for the equivalent solution. Conventional internal standardization will not suffice in this case, because of the differences in transport and dissociation behaviour between the analytes in the slurry particles and in the internal standard. Instead, a series of slurries can be analysed using both dissolution and slurry nebulization, and thus correction values can be computed empirically and later applied to unknown slurries. However, such a method relies on similar behaviour among all the slurries investigated.

7. Fundamental studies

At present, several fundamental studies on the transport and evaporation behaviour of slurry particles made of refractory materials in plasma have been reported. Wang *et al.*[60,61] investigated the changes in excitation temperature and electron density of the plasma when TiO_2 5 wt% slurry was nebulized in an ICP torch. No obvious changes in the excitation temperature or electron density were observed in the torch tunnel compared to those obtained for aqueous nebulization

for introduction into the plasma.

7.1 Plasma parameters

Slurry vaporization depends on the fundamental properties of plasmas, so a complete understanding of the ICP is desirable. Several studies on the fundamental ICP parameters for solution nebulization have been reported.[62-64] However, to the best of our knowledge, there are few studies regarding the plasma parameters for slurry introduction. Both the excitation temperature and electron density in the plasma channel have been reported for TiO_2 5 wt% slurry nebulization.[60,61] The electron density of the plasma for titanium slurry nebulization was determined using the Stark broadening method for the H_β line (486.11 nm) and was found to be the same as for solution nebulization, near 10^{15} cm^{-3}. Similarly, the excitation temperatures were almost the same for both slurry and solution nebulization (~5000–6000 K). Thus, it can be concluded that no significant differences in the plasma parameters can be identified between the slurry and aqueous solution nebulization.

7.2 Transport behaviour of slurry particles

The sizes of the slurry particles transported to the plasma have been examined by some research groups. It was found that only the particles smaller than 10 μm could contribute to the analyte emission signal.[16] Very small particles preferentially migrate to the ICP torch through selective transport due to the order-sorting of the spray chamber and gravity effects. In order to measure the upper size limit of the particles transported to the torch and to distinguish the effects related to the transport behaviour of a particular material from those caused by evaporation, the particle size distribution of the original slurry and that after pneumatic nebulization have to be determined. The experiments conducted by Wang *et al.*[65] revealed that the particle size distribution of the powder collected at the torch outlet was significantly different from that of the original powder. Their results were in good agreement with those reported by Ebdon.[67] Currently, it is only clear that particles with sizes smaller than 10 μm can reach the plasma.

7.3 Evaporation behaviour of slurry particles

Complete evaporation is difficult to achieve in the plasma for most advanced ceramic materials because of their extremely stable thermal properties, and thus the measured results can be lower than the real values. Therefore, an understanding of the evaporation behaviour of slurry particles in the plasma is highly desirable. Merten *et al.*[67] proposed and developed a model for estimating the evaporation behaviour. Their model predictions were verified by experimental results,

particularly for Al_2O_3. However, for SiC, the model predictions deviated from the experimental values, indicating that the evaporation process is still not completely understood. Lim *et al.*[68] investigated the vaporization process of SiO_2 particles in an ICP both theoretically and experimentally. The Si I line emission intensities were measured as a function of observation height for three SiO_2 slurry samples with different particle sizes. Under the assumption that the height was related to the vaporization time, the heat-transfer and mass-transfer evaporation models proposed by Hieftje and co-workers[69] were adopted to understand the vaporization mechanism. The simulation results confirmed that SiO_2 particles with sizes in the range of 0.3–2.6 nm were completely vaporized in atmospheric-pressure ICP through a heat-transfer-controlled mechanism rather than a Knudsen-effect-corrected heat-transfer-controlled or mass-transfer-controlled mechanism. The upper size limit for the particles that can be evaporated completely in the plasma was also determined. Wang *et al.*[23] studied the relationship between the percentage of Al_2O_3 slurry powders vaporized and the particle size. The maximum Al_2O_3 particle size for complete vaporization in the plasma is about 7 μm. The vaporization efficiency decreased with increasing particle size, and only about 46% of the particle mass was vaporized for a particle size of 10 μm.

8. Applications

Some recent applications of advanced ceramics slurry nebulization introduction into plasma for trace element determination are listed in Table 3. These applications are listed alphabetically for sample type, and the elements determined, the analytical technique used, and calibration techniques are given. A wide range of applications to various advanced ceramic materials is clearly evident, showing that slurry nebulization is applicable widely for the analysis of various ceramics.

9. Conclusions

Many reports have shown that up to now, slurry nebulization into the plasma for ICP spectrometry is the most mature method among solid sample introduction techniques, because only a simple modification of the nebulizer is needed.

Ceramic samples should be ground into micron-sized or even submicron-sized particles and prepared as a slurry with an appropriate amount of a stabilization agent. In theory, addition of the stabilization agent increases the zeta potential between the particles in the chosen medium to improve the slurry stability. A zeta potential of zero means that the slurry particles will agglomerate, and thus the slurry is unstable.

Furthermore, a suitable calibration method should be carefully selected. Establishing a series of standard materials with the same composition and particle size distribution would be ideal, but it is almost impossible. The use of aqueous solution standards seems attractive, but it is suitable only when the slurry particles completely evaporate in the plasma. An intrinsic internal standard method can be used to derive a correction coefficient only when the matrix and all analytes evaporate with nearly the same efficiency.

Because of this lack of a standard procedure, new methods will become necessary as new advanced ceramics are developed. In particular, the evaporation behaviours of different ceramics with different particle sizes in the plasma should be studied to successfully apply slurry nebulization introduction.

Acknowledgements

The financial support by the NSFC (20705036) and from the Plan of Creative Funding (SCX0626) is gratefully acknowledged.

References

1 J. A. C. Broekaert, T. Graule, H. Jenett, G. Tolg, P. Tschopel, *Fresenius J. Anal. Chem*., 1989, **332**, 825-838.
2 G. A. Hutchins, G. H. Maher, S. D. Ross, *Am. Ceram. Soc. Bull.*, 1987, **66**, 681-684.
3 M. Jayaratna, M. Yoshimura, S. Somiya, *J. Mater. Sci.*, 1987, **22**, 2011-2016.
4 D. Merten, J. A. C. Broekaert, R. Brandt, N. Jakubowski, *J. Anal. At. Spectrom.*, 1999, **14**, 1093-1098.
5 N. Tzenov, M. W. Barsoum, T. E. Raghy, *J. Eur. Ceram. Soc.,* 2000, **20**, 801-806.
6 M. T. Larrea, I. G. Pinilla, J. C. Farinas, *J. Anal. At. Spectrom.*, 1997, **12**, 1323-1332.
7 E. D. Salin, G. Horlick, *J. Anal. Chem*., 1979, **51**, 2284-2286.
8 C. Skinner, E. Salin, *J. Anal. At. Spectrom.*, 1997, **12**, 725-732.
9 G. C. Y. Chan, M. N. Fan, W. T. Chan, *Spectrochim. Acta Part B*., 2001, **56**, 13-25.
10 H. Zhou, Z. Wang, Y. Zhu, Q. Li, H. J. Zou, *Spectrochim. Acta Part B*., 2013, **90**, 55-60.
11 J. Pisonero, B. Fernandez, D. Gunther, *J. Anal. At. Spectrom.*, 2009, **24**, 1145-1160.
12 R. E. Shane, A. L. Bruinen, R. M. A. Heeren. *Anal. Bioanal. Chem*., 2014, **406**: 1275-1289.
13 H. Nickel, Z. Zadgorska, *Fresenius J. Anal. Chem*., 1995, **351**, 158-163.
14 M. Resano,F. Vanhaeckeand M. T. C. de Loos-Vollebregt, *J. Anal. At. Spectrom*., 2008, **23**, 1441-1556.
15 J. C. Farinas, R. Moreno, J. M. Mermet, *J. Anal. At. Spectrom*., 1994, **9**, 841-849.
16 L. Ebdon, M. Foulkes, K. Sutton, *J. Anal. At. Spectrom*., 1997, **12**, 213-229.
17 M. C. Santos, J. A. Nobrega, *Appl. Spectrosc. Rev*., 2006, **41**, 427-448.
18 Z. Wang, Z. M. Ni, D. R. Qiu, G. Y. Tao, P. Y. Yang, *J. Anal. At. Spectrom.*, 2005, **20**, 315-319.

19 Z. Wang, Z. M. Ni, D. R. Qiu, G. Y. Tao, P. Y. Yang, *Anal. Chim. Acta*, 2006, **577**, 288-294.

20 D. M. Wu, H.Y. Qu, M. Dong, A. B. Wang, P. G. He, Y. Z. Fang, *Anal. Bioanal. Chem*., 2007, **389**, 2003-2008.

21 M. C. Santos, J. A. Nobrega, *J. Anal. At. Spectrom*., 2007, **22**, 93-96.

22 Z. Wang, D. R. Qiu, G. Y. Tao, P. Y. Yang, *J. Anal. At. Spectrom*., 2009, **24**, 1258-1261.

23 Z. Wang, J. Y. Zhang, H. J. Zou, M. Dong, D. R. Qiu, P. Y. Yang, *Talanta*, 2013, **107**, 338-343.

24 Z. Wang, Z. M. Ni, D. R. Qiu, T. Y. Chen, G. Y. Tao, P. Y. Yang, *J. Anal. At. Spectrom*., 2004, **19**, 273-276.

25 Z. Wang, Z. M. Ni, D. R. Qiu, G. Y. Tao, P. Y. Yang, *Spectrochim. Acta Part B*., 2005, **60**, 361-367.

26 H. Isoyama, Y. Uchida, T. Nagashima, O. Ohira, *J. Anal. At. Spectrom*., 2004, **19**, 1370-1374.

27 J. Goulter, *T IZ Int. Powder Bulk Mag*., 1992, **116**, 41-45.

28 C. Suryanarayana, *Progr. Mater. Sci.*, 2001, **46**, 1–184.

29 F. Vanhaecke, M. Resano, L. Moens, *Anal. Bioanal. Chem*., 2002, **374**, 188 -195.

30 G. D. Parfitt, *Appled science publishers*, New York, 1981.

31 I. Varga, F. Csempesz, G. Zaray, *Spectrochim. Acta Part B*., 1996, **51**, 253-259.

32 B. Hu, S. Q. Li, G. Q. Xiang, M. He, Z. C. Jiang, *Appl. Spectrosc. Rev*., 2007, **42**, 203-234.

33 L. Ebdon, A. R. Collier, *J. Anal. At. Spectrom*., 1988, **3**, 557-561.

34 M. Huang, X.-E. Shen, *Spectrochim. Acta, Part B*, 1989, **44**, 957-964.

35 G. L. Long, I. B. Brenner, *J. Anal. At. Spectrom*., 1990, **5**, 495-499.

36 J. A. C. Broekaert, F. Leis, B. Raeymaekers, G. Zaray, *Spectrochim. Acta, Part B*, 1988, **43**, 339-353.

37 S. A. Darke, S. E. Long, C. J. Pickford, J. F. Tyson, *Fresenius J. Anal. Chem*., 1990, **337**, 284-289.

38 L. S. Gervais, E. D. Salin, *J. Anal. At. Spectrom*., 1991, **6**, 41-47.

39 G. Zaray, I. Varga, T. Kantor, *J. Anal. At. Spectrom.*, 1994, **9**, 707-712.

40 I. Varga, G. Zaray, J. Szepvolgyi, G. Konya, *Mikrochim. Acta*, 1989, **3**, 381-387.

41 J. A. C. Broekaert, C. Lathen, R. Brandt, C. Pilger, D. Pollman, P. Tschopel, G. Tolg, *Fresenius J. Anal. Chem*., 1994, **439**, 20-25.

42 R. Lobinski, W. V. Borm, J. A. C. Broekaert, P. Tschopel, G. Tolg, *Fresenius J. Anal. Chem*., 1992, **342**, 563-568.

43 G. A. Zachariadis, C. E. Michos, J. *Pharmaceutical Biomed. Anal*., 2007, **43**, 951-958.

44 G. A. Zachariadis, L. I. Valianou, *Appl. Spectrosc*., 2008, **62**, 716-720.

45 Z. Wang, J. Y. Zhang, D. R. Qiu, H. J. Zou, H. Y. Qu, Y. R. Chen, P. Y. Yang, *J. Anal. At. Spectrom*., 2010, **25**, 1482-1484.

46 L. Ebdon, J. R. Wilkinson, *J. Anal. At. Spectrosc.*, 1987, **2**, 39-44.

47 C. W. Fuller, R. C. Hutton, B. Preston, *Analyst*, 1981, **106**, 913-920.

48 W. V. Borm , J. A. C. Broekaret, *Anal.Chem*.,1990, **62**, 2527-2532.

49 L. Ebdon, M. E. Foulkes, H. G. M. Parry, C.T. Tye, *J. Anal. At. Spectrom*., 1988, **3**, 753-761.

50 L. Ebdon, A. R. Collier, *Spectrochim. Acta Part B*.,1988, **43**, 355-369.

51 J. H. D. Hartley, S. J. Hill, L. Ebdon, *Spectrochim. Acta Part B*.,1993, **48**, 1421-1433.

52 B. Kollander, M. Andersson, J. Pettersson, *Talanta,* 2010, **80**, 2068-2075.

53 J. G. Williams, A. L. Gray, P. Norman, L. Ebdon, *J. Anal. At. Spectrom*., 1987, **2**, 469-472.

54 C. Xhoffer, C. Lathen, W. V. Borm, J. A. C. Broekaert, W. Jacob, R. V. Grieken, *Spectrochim. Acta, Part B*, 1992, **47**, 155-172.

55 M. L. Fernandez, B. Fairman, A. S. Medel, *J. Anal. At. Spectrom*., 1991, **6**, 397-401.

56 C. Chen, T. W. Mccreary, *Appl. Spectros*., 1994, **48**, 410-412.

57 M. Totland, I. Jarvis, K. E. Jarvis, *Chem. Geol.*, 1993, **104**, 175-188.

58 L. Marjanovic, R. I. McCrindle, B. M. Botha, H. J. Potgieter, *Anal. Bioanal. Chem*., 2004, **379**, 104-109.

59 T. Mochizuki, A. Sakashita, H. Iwata, Y. Ishibashi, N. Gunji, Anal. Sic.,1989,5.311-317.

60 Z. Wang, D. R. Qiu, G. Y. Tao, P. Y. Yang, *Spectrosc. Spectral Anal.*, 2009, **29**, 793-797.

61 Z. Wang, D. R. Qiu, G. Y. Tao, P. Y. Yang, *Spectrosc. Spectral Anal*., 2009, **29**, 1402-1413.

62 P. Yang, R. M. Barnes, J. Mostaghimi, M. I. Boulos, *Spectrochim. Acta Part B*., 1989, **44**, 657-666.

63 P. Yang, J. A. Horner, N. N. Sesi, G. M. Hieftje, *Spectrochim. Acta Part B*., 2000, **55**, 1833-1845.

64 H. Lindner, A. Murtazin, S. Groh, K. Niemax, A. Bogaerts, *Anal. Chem*., 2011, **83**, 9260-9266.

65 J. Y. Zhang, Z. Wang, Y. P. Du, D. R. Qiu, P. Y. Yang, *Chinese J. Anal. Chem*., 2011, **39**, 658-663.

66 S. Sparkes, L. Ebdon, *Anal. Proc*., 1986, **23**, 410-423.

67 D. Merten, P. Heitland, J. A. C. Broekaert, *Spectrochim. Acta Part B*., 1997, **52**, 1905-1922.

68 H. B. Lim, T. H. Kim, S. H. Eom, Y. I. Sung, M. H. Moon, D. W. Lee, *J. Anal. At. Spectrom*., 2002, **17**, 109-114.

69 J. A. Horner, G. C.Y. Chan, S. A. Lehn, G. M. Hieftje, *Spectrochim. Acta Part B*., 2008, **63**, 217-233.

70 T. Y. Peng, G. Chang, L. Wang, Z. C. Jiang, B. Hu, *Fresenius J. Anal. Chem*., 2001, **369**, 461-465.

71 B. U. Peschel, F. Andrade, W. C. Wetzel, G. D. Schilling, G. M. Hieftje, J. A. C. Broekaert, R. Sperline, M. B. Denton, C. J. Barinaga, D. W. Koppenaal, *Spectrochim. Acta, Part B*, 2006,**61**, 42-49.

72 M. C. Wende, J. A. C. Broekaert, *Spectrochim. Acta, Part B*, 2002,**57**, 1897-1904.

73 J. Mierzwa, M. H. Yang, *J. Anal. At. Spectrom*., 1998, **13**, 667-671.

74 M. C. Wende, J. A. C. Broekaert, *Fresenius J. Anal. Chem*., 2001, **370**, 513-520.

75 M. A. Amberger, J. A. C. Broekaert, *J. Anal. At. Spectrom.,* 2010, **25**, 1308-1315.

76 P. Barth, J. Hassler, I. Kudrik, V. Krivan, *Spectrochim. Acta, Part B*, 2007, **62**, 924-932.

77 S. M. Cristina dos, N. A. Rita A, N. J. de Araújo, *J. Mex. Chem. Soc*., 2005, **49**,134-137.

78 S. Q. Li, B. Hu, Z. C. Jiang, *J. Anal. At. Spectrom*., 2004,**19**,387-391.

79 J. Hassler, G. Zaray, K. Schwetz, K. Florian, *J. Anal. At. Spectrom*., 2005, **20**, 954-956.

80 T. Y. Peng, G. Chang, X. H. Sheng, Z. C. Jiang, B. Hu, *Anal. Chim. Acta*, 2001, **433**, 255-262.

81 T. Y. Peng, X. H. Sheng, B. Hu, Z. C. Jiang, *Analyst*, 2000, **125**, 2089-2093.

82 U. Schaffer, V. Krivan, *Anal. Chem*., 1999, **71**, 849-854.

83 T. Y. Peng, Z. C. Jiang, B. Hu, Z. H. Liao, *Fresenius J. Anal. Chem*.,1999, **364**, 551-555.

84 T. Y. Peng, Z. C. Jiang, Y. C. Qin, *J. Anal. At. Spectrom*.,1999, **14**, 1049-1053.

85 K. H. Kim, H. Y. Kim, H. B. Lim, *Bull. Korean Chem. Soc.*, 2001, **22**, 159-163.

86 Z. Wang, T. Y. Chen, G. Y. Tao, P. Y. Yang, *Spectrosc. Spectral Anal.*, 2005, **25**, 556-559.

87 T. Y. Peng, P. W. Du, B. Hu, Z. C. Jiang, *Anal. Chim. Acta*, 2000, **421**, 75-81.

88 T. Y. Peng, Q. Yan, B. Hu, Z. C. Jiang, *Chem. J. Chinese. U.*, 2000, **21**, 694-697.

89 M. Aramendia, M. Resano, F. Vanhaecke, *J. Anal. At. Spectrom*. 2009,**24**, 41-50.

90 S. Z. Chen, T. Y. Peng, Z. C. Jiang, *Anal. Lett*., 1999, **32**, 411-416.

Table 1 Grinding methods used in the preparation of slurries for introduction into plasma

Grinding method	Sample	Grinding time	Resulting particle size (μm)	Ref.
Bottle and bead	Silicon carbide	24 h	~7.9	19
Vibration mill	Magnesium niobate	2 h	0.6	20
	Clay and refractory	30 min	<37	21
	Boron carbide	3 min	1.9	22
	Silicon carbide	2 min	~1.5	19
Puck-type grinder	Aluminium oxide	3 min	0.5	23
	Titanium dioxide	2 min	<15	24
	Titanium nitride	2 min	~4.9	25
Jet milling	Boron carbide	/	0.5	22
Ultrasonic grinding method	Zirconium oxide-Aluminium oxide	10 min	0.5–0.7	26
Grinding mill	Silicon carbide	10 min	< 38	27

Table 2 Dispersants used to stabilize slurries for nebulization into plasmas

Dispersant	Concentration	Sample	Ref.
Ammonia	0.35% v/v	Kaolin clay	33
Darvan-7	0.5% m/m	Ceramics	15
Darvan-C	0.5% m/m	Ceramics	15
Dolapix PC-33	0.5% m/m	Ceramics	15
Glycerine+0.5 M HCl	40%	Zirconium oxide	34
Glycerol+Kodak photoflow	40% v/v 2% v/v	Ceramic, geological and refractory materials	35
Sodium hexametaphosphate	0.1% m/v	Refractory samples, sulphide ore	35
Sodium hexametaphosphate+ monoisopropanolamine	0.1% m/v	Titanium dioxide	36
Tetrasodium pyrophosphate	0.1% m/v	Silicon nitride	37

Triton X-100	0.01% v/v	Sediments	38
		Silicon carbide	27
HCl	1% m/m	Silicon nitride	39
NH_4PAA	0.5% m/m	Aluminium oxide	23
PEI	0.5% m/m	Silicon carbide	19
NH_4PAA	2% m/m	titanium nitride	25
PEI	0.8% m/m for μm size 2% m/m for nm size	Aluminium nitride	18
NH_4PAA	0.5% m/m for μm size 1.5%m/m for nm size	Titanium dioxide	24
None		Silicon nitride	40
		Aluminium oxide	41
		Silicon carbide	41
		Zirconium oxide	42
		Boron carbide	22

Table 3 Recent applications of slurry sampling ICP-OES for trace element determination

Sample	Analyte	Detection technique	Calibration	Ref
Aluminium nitride	Cr, Cd, Cu, Fe, Mg, Mn, Ni, P, Si, Ti, Y, Zr	ICP-OES	Aqueous standards, calibration curve method	18
Aluminium oxide	Cr, Cu, Fe, V	ETV-ICP-OES	Aqueous standards, standard addition method	70
Aluminium oxide	Cu, Fe, Ga	ETV- ICP-MS	Aqueous standards, standard addition method	71
Aluminium oxide	Ca, Fe, Ga, Mg, Mn, Na, Ni, V	ETV-ICP-OES	Aqueous standards, standard addition method	72
Aluminium oxide	Cr, Cu, Ga, Fe, Mg, Mn, Na, V, Zn	ETV-ICP-MS	Aqueous standards, standard addition method	73

Aluminium oxide	Ca, Fe, Ga, Mg, Mn, Na, Ni, V	ETV-ICP-MS	Aqueous standards, standard addition method	74
Boron carbide	Al, Ca, Cr, Cu, Fe, Mg, Mn, Na, Ni, Si, Ti, V, Zr	ICP-OES	Aqueous standards, calibration curve method	22
Boron carbide	Al, B, Ca, Fe, Ti	ETV-ICP-OES/MS	Aqueous standards, calibration curve method	75
Boron nitride	Al, Ca, Cr, Cu, Fe, Mg, Mn, Si, Ti, Zr	ETV-ICP-OES	Aqueous standards, calibration curve method	76
Ceramic powder	Al, B, Na, Mg, Ca, Ti, V, Cr, Mn, Fe, Co, Ni, Cu, Zn, Ga, Zr, Ba, La, Ce	ICP-OES/MS	Aqueous standards, calibration curve method	41
Clay and refractory materials	Al, Ca, Fe, K, Mg, P, Si, Ti	ICP-OES	Aqueous standards, calibration curve method	77
Clay and refractory materials	Al, Ca, Fe, K, Mg, Na, P, Si, Ti,	ICP-OES	Aqueous standards, standard addition method	21
Magnesium niobate	Ba, Ca, Cr, Cu, Fe, Mn, Ni, Pb	ICP-OES	Aqueous standards, calibration curve method	20
Niobium(V) oxide	Cu, Cr, Mn, Ni, Ta, Ti, W	ETV-ICP-MS	Aqueous standards, standard addition method	78
Silicon carbide	Al, Ca, Cr, Cu, Fe, Mg, Mn, Ni, Ti, V	ICP-OES	Aqueous standards, calibration curve method	45
Silicon carbide	Al, Ca, Cr, Cu, Fe, Mg, Mn, Ni, Ti	ICP-OES	Solid standards, standard addition method	19
Silicon carbide	Al	ETV-ICP-OES	Solid standards, standard addition method	79
Silicon carbide	B, Mo, Ti, Zr	ETV-ICP-OES	Aqueous standards, standard addition method	80
silicon carbide	Al, Cr, Cu, Fe, V	ETV-ICP-OES	Aqueous standards, both standard	81

			addition method and calibration curve method	
Silicon carbide, graphite	Al, Ag, As, Bi, Ca, Co, Cr, Cu, Fe, Ga, K, Li, Mg, Na, Ni, Pb	ETV-ICP-OES	Aqueous standards, calibration curve method	82
Silicon nitride powders	Cu, Cr, Ti, Al, Y	ETV-ICP-OES	Aqueous standards, calibration curve method	83, 84
Silicon nitride ultra-fine powder	Ca, W, Co, Al, Fe, Mg, Na	ICP-OES	Aqueous standards, calibration curve method	85
Titanium dioxide	Al, Ca, Cr, Fe, Mg, P, Pb, V, K, Si, Nb	ICP-OES	Aqueous standards, calibration curve method	24, 86
Titanium dioxide	Cr, Cu, Fe, V, Y	ETV-ICP-OES	Aqueous standards, standard addition method	87, 88
Titanium dioxide	As, Cd, Hg, Pb, Sb, Zn	ETV- ICP-MS	Aqueous standards, both standard addition method and calibration curve method	89
Titanium nitride	Ca, Cr, Fe, Mg, Ni, Si, Ti, Zr	ICP-OES	Aqueous standards, calibration curve method	25
Titanium nitride	Ca, Cr, Fe, Mg, Ni, Si, Zr, Ti	ICP-OES	Aqueous standards, calibration curve method using intrinsic internal standard	25
Zirconium oxide	La, Eu, Y	ETV-ICP-OES	Aqueous standards, calibration curve method	90
Zirconium oxide-Aluminium oxide	Zr, Al, Hf, Y, Ca, Fe, Mg, Mn, Ti	ICP-OES	Aqueous standards, calibration curve method	26

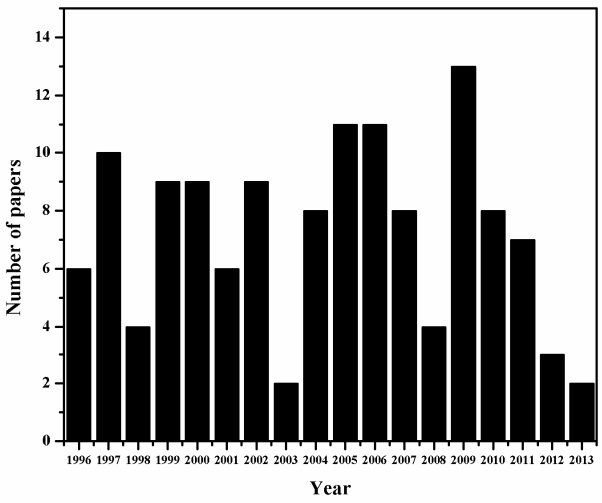

Fig.1 Number of papers published per year from 1996 to 2013 on slurry nebulization into plasma.

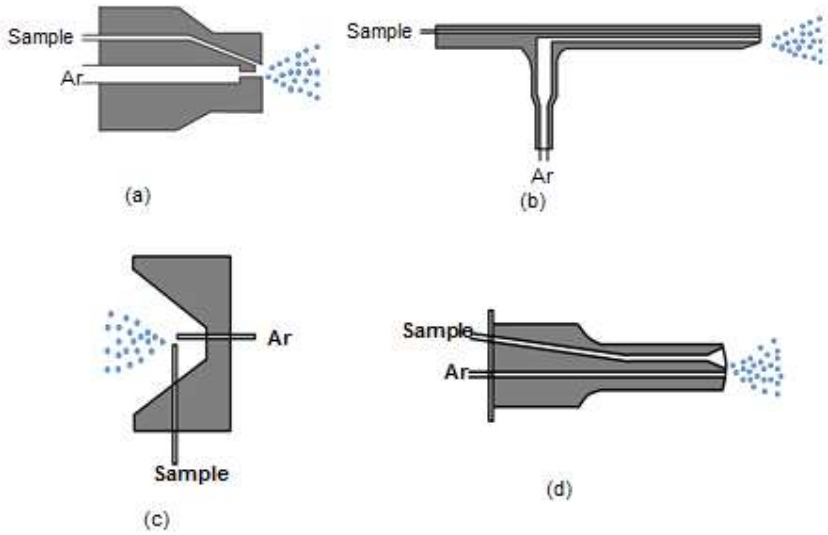

Fig. 2 Structural schematics of several nebulization devices: (a) V-groove Babington-type, (b) glass expansion concentric type, (c) cross-flow type, and (d) Burgener type nebulizers.

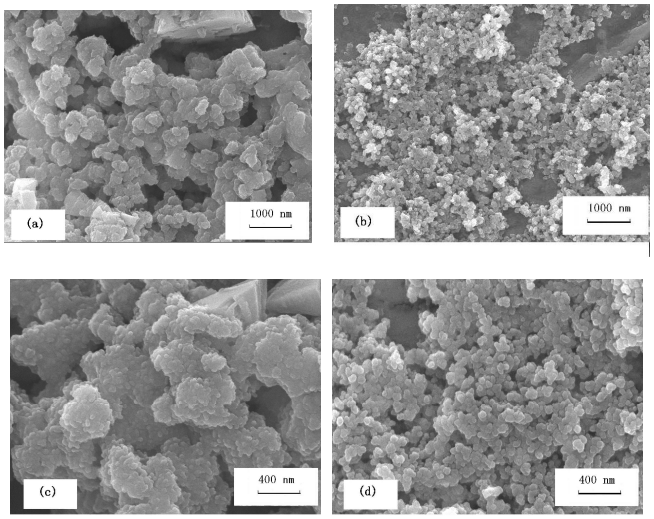

Fig. 3 SEM micrographs of sediments from a 2 wt.% AlN nanoparticle suspension at pH 6.0 (a) without dispersants at ×20000, (b) with dispersants at ×20000, (c) without dispersants at ×50000, and (d) with dispersants at ×50000. （Reprinted with permission from ref. 18. Copyright 2005, Royal Society of Chemistry）

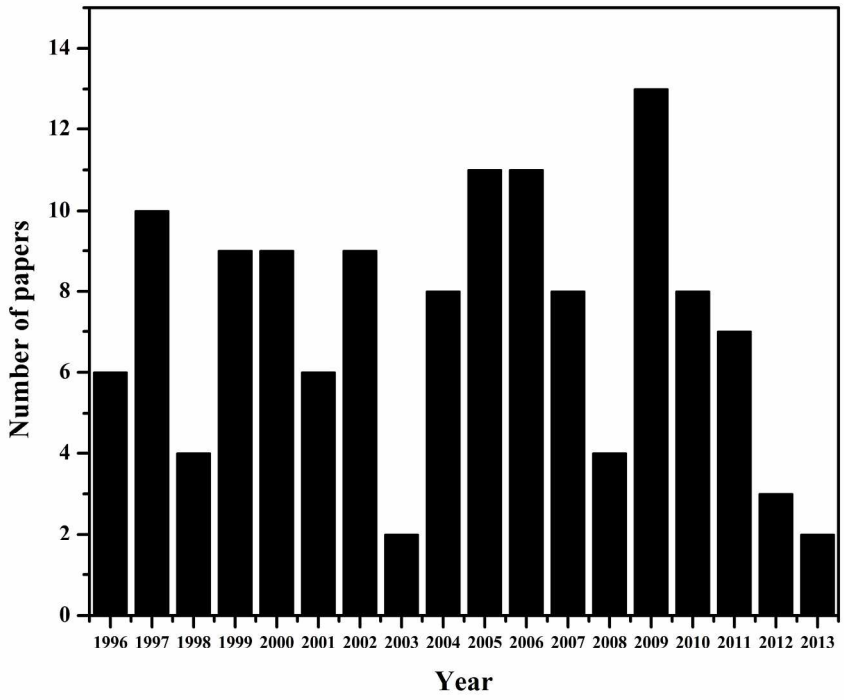

Fig.1 Number of papers published per year from 1996 to 2013 on slurry nebulization into plasma.
218x187mm (300 x 300 DPI)

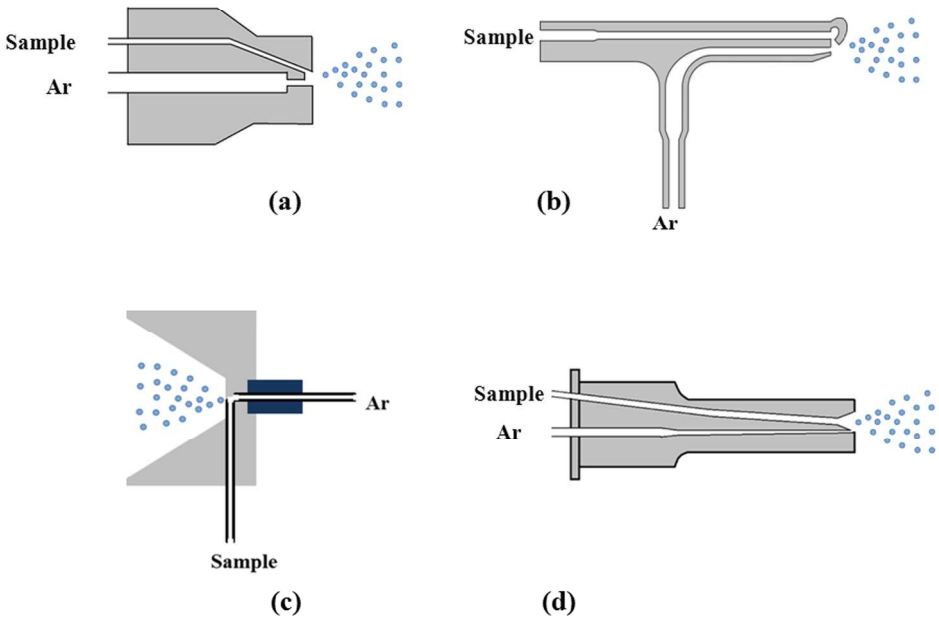

Fig.2 Structural schematics of several nebulization devices: (a) V-groove Babington-type, (b) glass expansion concentric type, (c) cross-flow type, and (d) Burgener type nebulizers.
190x142mm (300 x 300 DPI)

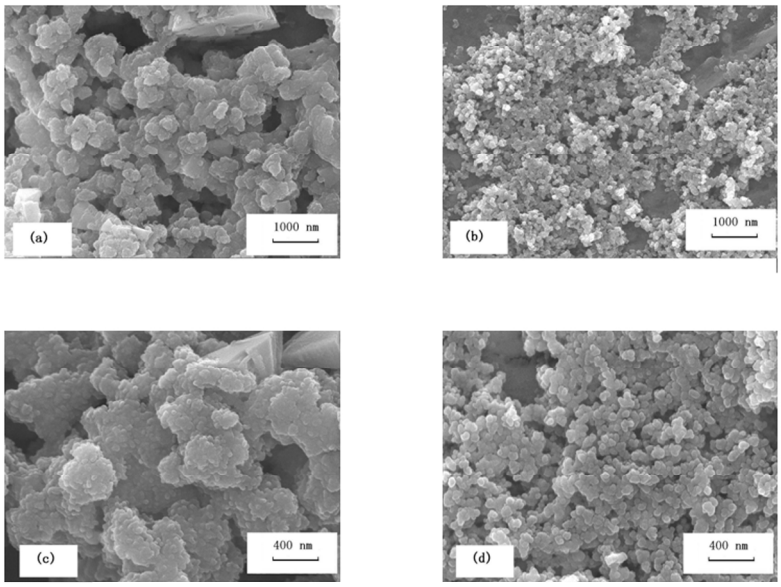

Fig.3 SEM micrographs of sediments from a 2 wt.% AlN nanoparticle suspension at pH 6.0 (a) without dispersants at ×20000, (b) with dispersants at ×20000, (c) without dispersants at ×50000, and (d) with dispersants at ×50000.（Reprinted with permission from ref. 18. Copyright 2005, Royal Society of Chemistry）
190x142mm (300 x 300 DPI)